

ORIGINAL ARTICLE

Newtype large Rashba splitting in quantum well states induced by spin chirality in metal/topological insulator heterostructures

Ching-Hao Chang^{1,4}, Tay-Rong Chang^{2,4} and Horng-Tay Jeng^{2,3}

In a two-dimensional system without inversion symmetry, such as a surface or interface, the potential-asymmetry-induced electric field can create the Rashba effect, which is spin-band splitting caused by spin-orbit coupling (SOC). On the basis of Rashba splitting, several promising spintronic devices, such as the Datta-Das spin transistor, have been designed for manipulating spin precession in the absence of a magnetic field. Rashba splitting can be created in several metal quantum well states (QWSs), such as in Pb/Si; however, the effect is usually moderate because the itinerant carriers within the metal film strongly screen out the electric field. A large Rashba splitting can be found in the unoccupied QWSs of the Bi monolayer on Cu (111); however, the metallic substrate limits the diversity of its applications. To achieve strong Rashba splitting in metal thin film based on an insulating substrate, which is most desirable, we propose the normal metal (NM)/topological insulator (TI) heterostructure for manufacturing Rashba-type splitting in NM QWSs. In such a hybrid system, the TI spin-momentum-locking Dirac surface state associated with SOC strongly modifies the penetration depth of the NM QWS into the TI substrate according to the spin orientation, leading to strong Rashba-type splittings in the NM QWS. Combining *ab initio* calculations and analytical modeling, the momentum separation of the Rashba splitting in the NM QWS can be as large as 0.18 \AA^{-1} , which is the largest ever found in metal-film/non-metallic substrate systems. Furthermore, the induced spin polarization in the Rashba band is nearly 100%, much higher than the typical value of 40–50% in the TI surface state itself. This remarkably large Rashba splitting and the high spin polarization in the NM QWS evoked by the spin chirality of the TI surface state confer great potential for the development of spintronic devices.

NPG Asia Materials (2016) 8, e332; doi:10.1038/am.2016.173; published online 25 November 2016

INTRODUCTION

One of the major tasks in the development of semiconductor spintronics is finding a material with remarkable Rashba-type splitting to control the spin current. For example, the Datta-Das spin transistor,¹ proposed for more than 20 years, switches the spin current by controlling the magnitude of Rashba splitting of a two-dimensional electron gas in a semiconductor heterostructure.^{2–6} After decades of trials, the Datta-Das spin transistor has finally been experimentally realized recently.⁷ However, the mild splitting of the two-dimensional electron gas bands is inapplicable for spin transistors working at room temperature or designed in the nanoscale.^{7–9} A much more feasible approach is thus highly desirable.

Alternatively, giant Rashba splittings can be found in the surface state (SS) of noble-metal-based surface alloys with strong spin-orbit couplings (SOCs) in heavy atoms.^{10,11} The interatomic electric field at the surface-alloy plane is the key to the giant splitting.¹² Regarding the influence of the metal host, the SS would be hidden in the spintronic functions; therefore, efforts have been made on searching for materials

with remarkable Rashba splittings for bulk carriers such as BiTeI (refs 13–16).

Metallic thin film is the building block for future nanotechnology, and quantum well states (QWSs) dominate its transport properties. Thus, Rashba or spin-band splittings created in QWSs over non-metallic substrates^{17–22} are of great industrial potential. However, it is a great challenge to create a remarkable Rashba splitting in NM QWSs because of the strong screening effect in the metallic film. For a film thicker than a few monolayers (MLs), the electronic structure is robust against the electric field applied at the boundaries.²³ The only exception is the significant splitting observed in the unoccupied QWS in the Bi ML over the metallic Cu(111) substrate.²²

To create the large Rashba-type splitting in the QWSs of metallic thin films on non-metallic substrates, we propose another physical source: the spin chirality at the boundary of a topological insulator (TI). The TI is a newly discovered phase of matter in which the chiral conducting channels, namely, the SOC caused spin-momentum-locking SSs, form at the boundaries of the bulk insulator and are

¹Research Center for Applied Sciences, Academia Sinica, Taipei, Taiwan; ²Department of Physics, National Tsing Hua University, Hsinchu, Taiwan and ³Institute of Physics, Academia Sinica, Taipei, Taiwan

⁴These authors contributed equally to this work.

Correspondence: Professor H-T Jeng, Department of Physics, National Tsing Hua University, 101 Section 2, Kuang Fu Road, Hsinchu 30013, Taiwan.

E-mail: jeng@phys.nthu.edu.tw

Received 15 March 2016; revised 4 July 2016; accepted 9 August 2016

protected by the time-reversal symmetry.^{24–35} For a normal metal (NM)/TI heterostructure, or equivalently NM/semiconductor with a chiral spin texture SS, the SOC in the TI has the role of the orbital-dependent magnetic field in an insulator,^{36,37} and allows the NM QWS with the same spin and chirality as the TI SS to penetrate deeper than that with opposite spin and chirality. Moreover, the hybridization between the TI SS and the NM QWS at the interface further boosts the difference between the penetration depths of the two spin species.^{17,18} As a consequence of the spin–momentum-dependent penetration depth and trapping width, Rashba-type splittings arise in the NM QWSs. The physical diagram is illustrated in Figure 1.

In this article, via combined first-principles calculations and analytical analyses, we propose a new type of large Rashba splitting in the NM QWS induced by the spin chirality of the Dirac SS in the TI substrate. We demonstrate that the momentum separation of the Rashba-like splitting in the Ag/Bi₂Se₃ junction is the largest value among previously reported values for metal QWSs over non-metallic substrates.^{13,14} Moreover, the spin polarization of the induced spin splitting in QWSs could be nearly 100%, which is even higher than the typical value of 40–50% in the Dirac bands of TIs such as Bi₂Se₃.^{38–40} Both properties are ideal for realizing spintronic devices at the nanoscale. To achieve the above-mentioned main goal of this work, we use the model system Ag/Bi₂Se₃ to demonstrate the spin splitting in Ag QWSs induced by the Bi₂Se₃ SS. From a theoretical viewpoint, the 4*d* transition metal Ag film with weaker SOC helps to clarify whether the SOC in the NM film or the interaction with the TI is the main driving force of the large Rashba splitting in the QWS. Practically, any type of NM or TI can fulfill the NM/TI heterostructure and the Rashba splitting in future experiments. Heavy elements such as Au, with strong SOC, could be intuitively an even better candidate.

MATERIALS AND METHODS

We perform first-principles calculations for the Ag(3–12 ML)/Bi₂Se₃(6QL) slab model using the full-potential projected augmented wave method^{41,42} as implemented in the Vienna Ab-initio Simulation Package (VASP)^{43,44} within the generalized gradient approximation.⁴⁵ The Ag(NML)/Bi₂Se₃(6QL) slab structure is optimized using a 11 × 11 × 1 Monkhorst-Pack *k*-point mesh over the two-dimensional irreducible Brillouin zone. SOC is included in the band structure calculations. In this paper, we show results of only the *N*=5 case

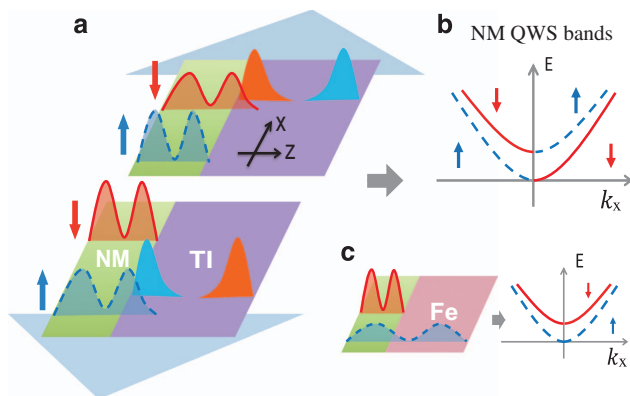


Figure 1 Spin-chirality-induced Rashba-type splitting in the NM–TI junction. (a) At the interface, the spin up (blue filled curve) and down (red filled curve) chiral TI edge states move in negative and positive *x* directions, respectively. The spin up (blue dashed curve) and down (red solid curve) NM QWS moving along $-x$ and $+x$ directions, respectively, penetrate deeply into the TI and reduce the band energies (see b). (c) A reference case of the effective Zeeman-type splitting induced by a ferromagnetic layer. NM, normal metal; QWS, quantum well state; TI, topological insulator.

because, in this case, the QWS energy crosses the SS bands within the Bi₂Se₃ bulk band gap, resulting in the maximum Rashba-like splitting among all the cases studied.

RESULTS AND DISCUSSION

To examine the proposed Rashba-type splitting in the NM/TI heterostructure depicted in Figure 1, the lattice structure, site-spin(in-plane)-decomposed band structures and the charge profiles of Ag(5 ML)/Bi₂Se₃ (6QL) from first-principles calculations are shown in Figure 2. The significant interaction between the TI SSs and the Ag QWSs lifts the energy degeneracy of the SSs at different sides of the Bi₂Se₃ layer. The Dirac point of the SS at the interface locates at approximately -0.6 eV, whereas at the surface side the Dirac point locates at approximately -0.4 eV. Because of the charge transfer from the Ag film on the Bi₂Se₃ substrate, the Dirac SSs (DSSs) show electron-doping behaviors. At the surface side, the band dispersion of the DSS (Figure 2d) is almost the same as that of the pristine Bi₂Se₃ DSS (Figure 2b). At the interface, the Bi₂Se₃ SS and the SOC strongly affect the Ag QWSs crossing the TI SSs approximately within the TI bulk band gap, giving rise to the giant Rashba-type spin splitting of the Ag QWSs at approximately -0.1 and -0.4 eV, as shown in Figure 2e (see the green dashed boxes K1 and K2). The induced strong energy separation in these spin-splitting Ag QWSs is ~ 0.35 eV (green vertical arrow in Figure 2e), which is indeed large compared with the Rashba energy parameter, E_R , of other reported systems listed in Supplementary Table S1.

Furthermore, the QWS–SS interaction strength exhibits significant spin dependency: the Ag QWS interacts strongly with the Bi₂Se₃ SS in the outer Rashba band (spin down along positive momentum in Figure 2e), whereas they hybridize only weakly in the inner Rashba band (spin up along positive momentum in Figure 2e). It can be observed in the top and middle panels of Figure 2f that the outer Rashba band (R1) is contributed by both the Ag QWSs and TI SSs, whereas the inner Rashba band (R2) is mainly the Ag QWSs. Because of the chiral spin texture of the Bi₂Se₃ SS, the Ag QWS with the correct spin chirality can penetrate deeper into Bi₂Se₃ (red curve in Figure 2f) and interact strongly with the TI SS with lower band energy (red line in the green boxes in Figure 2e), leaving the other spin chirality less hybridized with higher band energy (blue line in green boxes in Figure 2e). The QWS–SS interaction strength depends not only on the spin but also on the momentum, as shown in the top and middle panels of Figure 2f. The outer Rashba band (R1) wavefunction distributes mainly in the Bi₂Se₃ layer around the Γ -point (K1), whereas it locates mostly in the Ag layer away from the zone center (K2). This result demonstrates that the Ag QWS hybridizes with the TI SS strongly near the crossing point, whereas the hybridization strength decreases significantly beyond the zone center region.

A considerable Rashba splitting has been observed in the Ag SSs based on the Ag/Au junction.^{46,47} Because of the surface nature, the contributions of the Ag SSs on the transport properties are lower than those from the bulk-nature Ag QWSs. The spin-band splitting can commonly be described by the Bychkov–Rashba model $E_{\pm}(k_x) = \hbar^2 k_x^2 / (2m^*) \pm \alpha_R k_x$ ^{48,49} and the Rashba parameter can be estimated by $\alpha_R = \Delta E / (2k_x)$.³⁶ As indicated by the green vertical arrow in Figure 2e, the α_R obtained in our Ag QWS splitting reaches 1.75 eV Å, which is one order of magnitude larger than that of the Ag SS splitting. The industrial potential of the Ag QWS splitting in our Ag/Bi₂Se₃ junction is clearly much more promising.

Figure 3a shows a three-dimensional sketch of the upside-down bell-like energy surfaces of the Rashba bands (the R1 and R2 bands in Figure 2). The spin textures can be seen clearly in the projected two-dimensional energy contours in Figure 3b. At an energy near -0.3 eV,

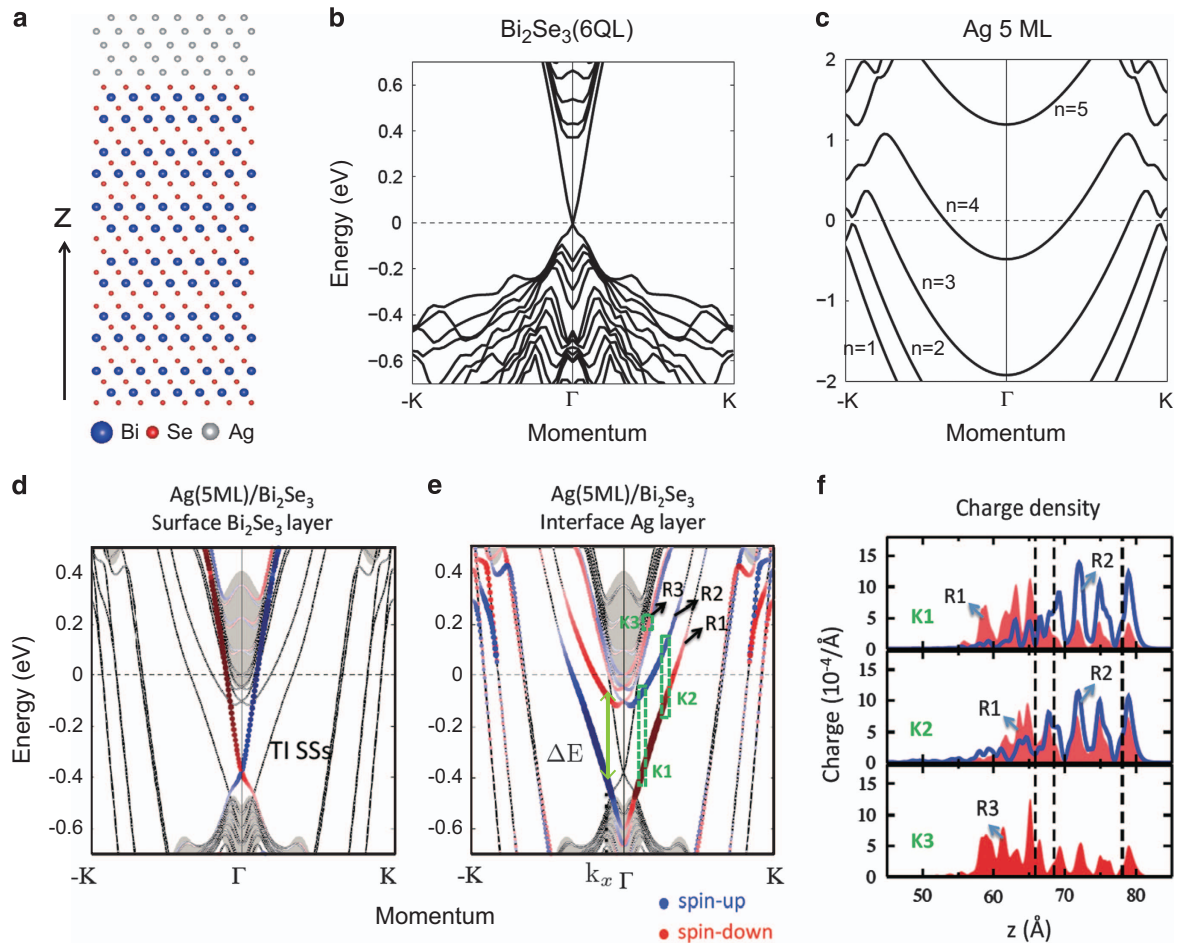


Figure 2 Lattice structure, band structures and charge profiles of Ag(5 ML)/Bi₂Se₃(6 QL). (a) Side view of the lattice structure of Ag(5 ML)/Bi₂Se₃(6 QL). The Ag–Ag and Ag–Se interlayer distances are 2.39 and 2.58 Å, respectively. (b, c) Band structures of free-standing Bi₂Se₃(6 QL) (b) and Ag(5 ML) (c) slabs. $n=1-4$ indicates the quantum numbers of the Ag QWSs. (d, e) In-plane spin polarization $\langle S_{x,y} \rangle$ of the Bi₂Se₃ surface state at the Bi₂Se₃ surface (d) and at the interface Ag (e). The brightness of the blue and red dots indicates the spin-up and -down components, respectively. R1 and R2 indicate the outer and inner Rashba bands, respectively. R3 denotes the TI SSs at the NM–TI interface. (f) Charge profiles of R1, R2 and R3 states with different momenta, as indicated in the green dash boxes in e. The vertical dashed lines from left to right indicate the positions of interface TI, interface Ag and surface Ag layers, respectively. NM, normal metal; QWS, quantum well state; TI, topological insulator.

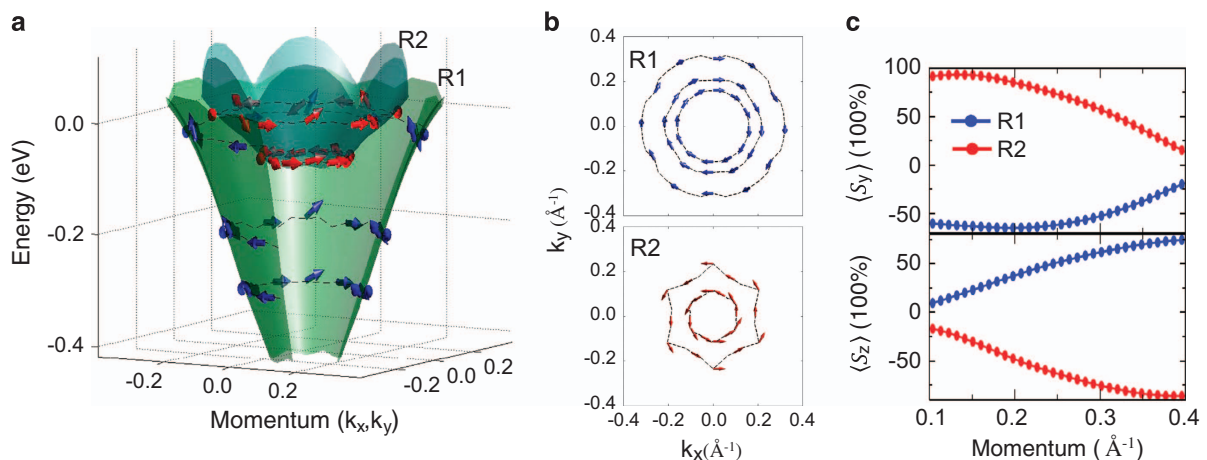


Figure 3 Three-dimensional band structures, spin textures and spin polarizations of the Rashba bands. (a) Energy surfaces and spin textures of the Rashba bands. (b) Top view of the spin textures. Blue (R1) and red (R2) arrows indicate the spin orientation over the outer and inner Rashba bands, respectively. (c) In-plane $\langle S_y \rangle$ (upper panel) and out-of-plane $\langle S_z \rangle$ (lower panel) spin polarizations of the Rashba bands along the k_x ($\Gamma - \bar{K}$) direction.

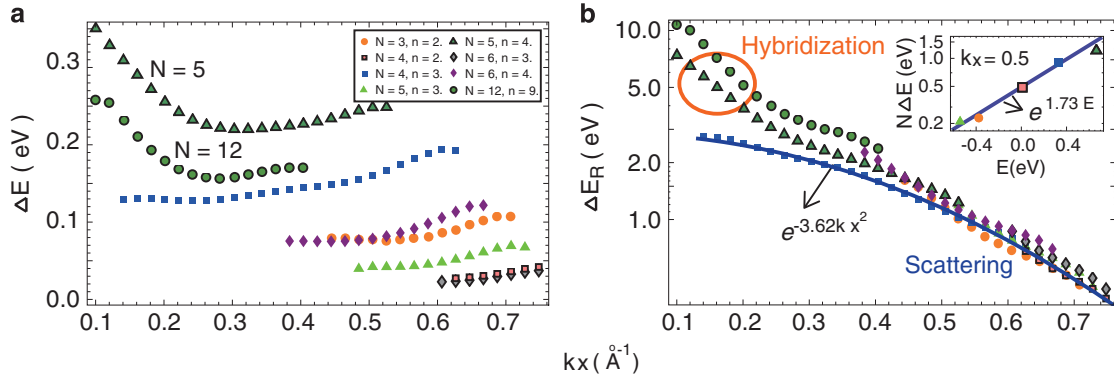


Figure 4 The spin gaps of the Rashba-type splitting in Ag QWSs as functions of the momentum. (a) The spin gap ΔE in Figure 2a for the n -th Ag QWSs in the Ag(NML)/Bi₂Se₃(6QL) junction. (b) The results in **a** are described by a universal formula $\Delta E \propto \exp(\alpha E - \beta k_x^2)$, as provided in equation (2). The α is obtained as 1.73 in the inner **b** by comparing results with fixing k_x but different E . β is found as 3.62 in outer **b** by defining $\Delta E_R = N\Delta E \exp(-1.73 E \text{ eV}^{-1})$. QWS, quantum well state.

the in-plane spin texture of R1 displays left-hand chirality similar to the pristine Bi₂Se₃ one (inner circle in the upper panel of Figure 3b). At a higher energy where the R1 and R2 bands coexist, the spin textures of the outer (R1) and inner (R2) bands circulate in the opposite directions, keeping the overall time-reversal symmetry. The contours at a high energy around the Fermi level (E_F) show hexagonal-type shapes with stronger warping because of higher order terms of SOC.⁵⁰

Spin polarization is one of the most important factors for high-efficiency spintronics. In contrast to the fully spin-polarized TI SSs demonstrated by early phenomenological models, recent experiments³⁸ and first-principles calculations³⁹ manifest relatively low spin polarizations of 40–50% for the Dirac states because of the strong spin-orbit entanglements that the spin polarizations from different orbitals can suppress the total polarization.^{38–40} As a result, searching for high spin polarization is urgently demanded. Figure 3c shows the spin polarization $\langle S_\alpha \rangle = \langle \sigma_\alpha \rangle / n_0$ of the Rashba bands along the k_x direction (Γ - \bar{K}), where σ is the spin component, $\alpha = x, y, z$ and n_0 is the occupation. Surprisingly, the induced in-plane spin polarizations $\langle S_{x,y} \rangle$ of the Rashba bands R2 and R1 around the Γ point ($k_x \sim 0.1 \text{ \AA}^{-1}$) are nearly 100% and 70%, respectively (Figure 3c, upper panel). Both cases overwhelm the recently observed value of $\sim 40\%$ in the Bi₂Se₃ DSS itself.³⁸ Away from the zone center, $\langle S_z \rangle$ emerges and reduces the in-plane spin polarizations. By contrast, for a large momentum, $k_x \sim 0.4 \text{ \AA}^{-1}$, the out-of-plane spin polarizations $\langle S_z \rangle$ of both the R2 and R1 bands also reach a very high value of $\sim 80\%$ (Figure 3c, lower panel). The high spin polarizations of these Ag QWSs are because of the single s -orbital character of the Ag QWSs, which results in reduced spin-orbital entanglements. Such entanglements drastically decrease the spin polarization in the multiorbital ($p_{x,y,z}$) TI DSSs. The multidirectional high spin polarizations could be manipulated by tuning both the E_F and the k -vector, yielding high-potential applications for spintronics.

Although the TI SSs induced spin splitting in the Ag QWSs is termed ‘Rashba-like bands’ in this work, the origin is entirely different from the traditional Rashba splittings stemming from the surface or interface electric fields. To clarify this issue, we examined a series of Ag thicknesses in Ag(NML)/Bi₂Se₃(6QL) junction with $N=3, 4, 5, 6, 10$ and 12 ML, and plotted the spin splitting ΔE of the Ag QWS for all these systems as functions of the momentum together in Figure 4a. In general, the remarkable Rashba-type splittings of Ag QWSs appear in all the studied cases (see also the Supplementary Figure S1). Surprisingly, the energy gap ΔE between two spin bands³⁶ is extremely

large with the magic thicknesses of 5 and 12 ML Ag, as shown in Figure 4a. These Rashba splittings can be explained by the combined hybridization and spin-dependent scattering mechanism. In the following, we first discuss the spin-dependent scattering at the NM–TI interface induced by the TI SOC, and then discuss the hybridization between the NM QWSs and the TI chiral spin DSSs.

For most junctions (except the 5 and 12 ML Ag cases), we prove in the following that their moderate Rashba-type splitting in the metallic QWS is solely generated by the spin-dependent reflection at the NM–TI interface. For an electron with effective mass m^* , energy E and momentum $\{k_x, k_z\}$ reflected by the substrate with a potential barrier V , the tunneling state is $\exp[-\gamma_z z + ik_x x]$ with decay constant

$$\gamma_z = \sqrt{2m^*(V - E)/\hbar^2 + k_x^2} \approx \frac{\sqrt{2m^*V}}{\hbar} \left(1 - \frac{E}{2V} + \frac{\hbar^2 k_x^2}{4m^*V} \right). \quad (1)$$

Here, the potential V approximates the effects from both the band offset between NM and TI layers, and the Schottky barrier at the NM–TI interface.⁵¹ We have used the condition $V \gg E$ in the above approximation, which is reasonable for the Ag/Bi₂Se₃ junctions. As the TI SOC causes the Rashba-type splitting by affecting the tunneling part of the metallic QWS, the spin gap ΔE defined in Figure 2a should be proportional to the tunneling amplitude in TI:

$$\Delta E \propto \frac{1}{Nm^*} e^{-W\gamma_z} \approx \frac{1}{Nm^*} e^{W\frac{\sqrt{2m^*V}}{\hbar}(-1 + \frac{E}{2V} + \frac{\hbar^2 k_x^2}{4m^*V})}. \quad (2)$$

Here, N is the thickness (ML) of the metallic slab and W is the interlayer distance between NM and TI layers. The spectra calculated with different interface spacing (W) are shown in Supplementary Figure S5a,b. Both the momentum offset k_0 and energy difference ΔE in the Rashba-type splitting decay exponentially with increasing interface spacing W (Supplementary Figure S5c), being consistent with equation (2). Below, we focus on the impact of the Ag thickness N with the geometrically optimized interlayer spacing $W \sim 2.6 \text{ \AA}$ in the junctions.

The prefactor $1/(Nm^*)$ obtained analytically from Supplementary equation S8 would suppress the weighting (impact) of the tunneling part in the NM QWS and reduce the energy separation upon increasing the NM thickness (electron-effective mass). The spin gap ΔE is an exponential growth of the energy E in equation (2). The slope of growth (Figure 4a) can be approximately fitted as 1.73 eV^{-1} in the Ag/Bi₂Se₃ junction (see inner panel in Figure 4b). Moreover, the splitting also exponentially decays with the square of momentum, and all moderate Rashba-type splittings can be described by a universal

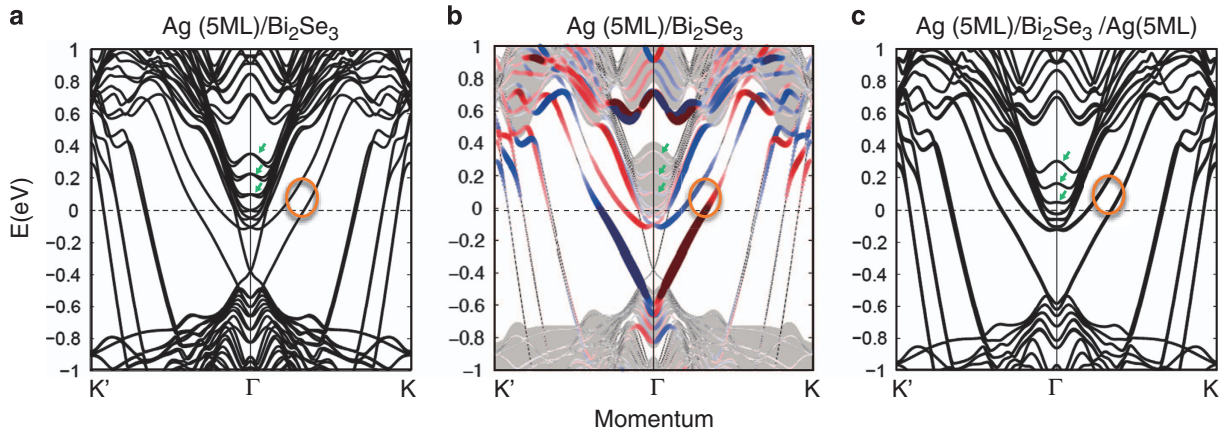


Figure 5 Band structures of Ag(5 ML)/TI bilayer (**a**, **b**) and Ag(5 ML)/TI/Ag(5 ML) trilayer (**c**). The green arrows indicate the traditional Rashba splittings induced by breaking the inversion symmetry. The orange circle indicates our proposed spin-chirality-induced Rashba splitting. (**b**) In-plane spin polarization $\langle S_{x,y} \rangle$ of states at the Bi_2Se_3 interface layer of the bilayer. In **c**, the traditional Rashba splittings in the TI states (green arrows) are eliminated, whereas the spin-chirality-induced Rashba-type splitting in the Ag QWSs (orange circle) remains nearly the same as that in **a**, **b**, QWS, quantum well state; TI, topological insulator.

formula, which is rescaled by defining $\Delta E_R = N\Delta E \exp(-1.73 E \text{ eV}^{-1})$, as shown in the outer panel in Figure 4b. As we increase the momentum in the Ag QWS, the energy part increases ΔE while the momentum part decreases ΔE . The competition between them results in a slight increment of ΔE upon increasing the momentum, as shown in Figure 4a. This trend is consistent with the spin-dependent reflection-induced Rashba-type splitting observed in $\text{Au}(111)/\text{W}(110)$ with strong SOC.³⁶ Here, we provide the first theory for this feature.

For junctions with magic thicknesses of 5 and 12 ML Ag, the splittings are extremely large, and ΔE grows again when the momentum is smaller than 0.2 \AA^{-1} , as shown in Figure 4a. In addition to the spin-dependent reflection that gives the overall increasing ΔE for larger k_x , the strong hybridization between the Ag QWS and the TI SS for small k_x is evidenced by the real space charge distribution shown in Figure 2f and Supplementary Figure S2c. The origin can be understood by the in-gap interaction between the Ag QWS and the TI SS in the momentum–energy space compared with Figure 2b–e. The strong hybridization occurs in $\text{Ag}(5 \text{ ML})/\text{Bi}_2\text{Se}_3$ as the $n=4$ Ag QWS (Figure 2c) shifts into the TI bulk band gap (Figure 2b) and interacts directly with the TI SS around the zone center (Figure 2d and e). The hybridization effect strongly drives the energy separation and leads to the giant splittings in the Ag QWS. Similarly, large Rashba splitting happens again in $\text{Ag}(12 \text{ ML})/\text{Bi}_2\text{Se}_3$ because another Ag QWS moves into the TI bulk band gap because of the thickness-dependent nature,⁵² as shown in the Supplementary Figure S1. Otherwise, the Ag QWS would also largely hybridize with the TI bulk bands and weaken the spin splitting as observed in the other cases (Supplementary Figures S1 and S2). For the R1 band (Figure 2d) close to the Γ point (K1, Figure 2e), the charge profile shown in the upper panel of Figure 2f is similar to the TI SSs (R3 in the lower panel of Figure 2f) that is modulated by the Ag overlayer.⁵³ Considering the hybridization effect, the increasing trend of the spin gap for $k_x < 0.2 \text{ \AA}^{-1}$ (Figure 4a) and the Rashba-type splitting near the Γ point (Figure 2e) can be well reproduced by the analytical method, as shown in the Supplementary Figure S4. However, as for the R1 band away from the zone center (also away from the TI SS), for example, around the Fermi level (K2 in Figure 2e), the R1 band is basically the Ag QWS modulated by the spin-dependent reflection at the TI interface. It can be seen clearly in the middle panel of Figure 2f that more than 60% of the spin-down electron cloud (red region)

locates inside the Ag layer. Moreover, the R2 and R3 bands are mainly the Ag QWSs and TI SSs, respectively, as evidenced by their charge-density profiles shown in Figure 2f.

In thin metal films, pure hybridizations between QWSs and SSs with huge Rashba splittings have been investigated intensively.^{17–19} The induced splittings in QWSs are not of the Rashba-type, and the spin gaps decrease dramatically when they leave the QWS SSs crossing points. Only with the combined effect from the strong in-gap hybridization for small k_x and the spin-dependent scattering for large k_x can the huge Rashba-type splitting in the Ag QWSs be generated over a large part of the Brillouin zone, which is proposed in this work for the first time.

To unambiguously demonstrate that the origin of the Rashba splitting in $\text{Ag}/\text{Bi}_2\text{Se}_3$ is indeed the strong interaction between Ag QWS and the chiral TI SS, we also explore Rashba splitting in the $\text{Ag}(5 \text{ ML})/\text{Bi}_2\text{Se}_3/\text{Ag}(5 \text{ ML})$ trilayer with the structure inversion symmetry, as shown in Figure 5. For the $\text{Ag}(5 \text{ ML})/\text{Bi}_2\text{Se}_3$ bilayer (Figure 5a and b), both the traditional Rashba splitting (green arrows) and our proposed new-type Rashba splitting (orange circle) coexist. As the traditional Rashba splitting is induced by breaking the structure inversion symmetry,^{54–56} it is thus eliminated in the $\text{Ag}(5 \text{ ML})/\text{Bi}_2\text{Se}_3/\text{Ag}(5 \text{ ML})$ trilayer (Figure 5c) with inversion symmetry, as indicated by the green arrows. By contrast, our proposed spin-chirality-induced Rashba-type splitting in the Ag QWSs of the $\text{Ag}(5 \text{ ML})/\text{Bi}_2\text{Se}_3/\text{Ag}(5 \text{ ML})$ trilayer (orange circle in Figure 5c) remains nearly the same as that in the $\text{Ag}(5 \text{ ML})/\text{Bi}_2\text{Se}_3$ bilayer (orange circle in Figure 5a and b). The only difference now is that the two surfaces at the TI spacer contain opposite spin chiralities. Therefore, the induced splittings become doubly degenerate with opposite spin polarizations on the Ag QWSs in the right- and left-hand side Ag cover layers.

To date, the largest splitting in occupied metal QWSs has been generated by the pure spin-dependent reflection in the $\text{Au}(111)/\text{W}(110)$.³⁶ The obtained Rashba parameter α is $\sim 0.16 \text{ eV \AA}$.³⁶ The largest value for Ag, $\alpha \approx 0.1 \text{ eV \AA}$ is found in the Ag SS on an Au substrate.^{46,47} In our proposed $\text{Ag}/\text{Bi}_2\text{Se}_3$ junction, the Rashba parameter, reaching 1.75 eV \AA in Figure 2e, is one order of magnitude larger than those in the above two systems. Furthermore, the momentum separation between two spin bands is important, for it directly determines the spin precession length and the minimum size of the spin transistor.¹ As shown in Figure 2e, the momentum

separation sensitively depends on energy that it increases from 0.14 to 0.18 \AA^{-1} along with the decreasing energy from E_F to -0.1 eV . Among all systems based on non-metallic substrates reported,^{13,14} our maximum momentum separation of 0.18 \AA^{-1} is the largest value ever reported (Supplementary Table S1).

Here, we emphasize that the giant momentum separation of 0.18 \AA^{-1} , obtained in a $\text{Ag/Bi}_2\text{Se}_3$ heterostructure, corresponds to a spin precession length of 1.7 nm, which would make the Datta-Das spin transistor possible at the nanoscale. Moreover, the large energy separation of 0.35 eV at E_F is an order of magnitude larger than the thermal energy $k_B T$ at room temperature. Thus, the generated spin current would be stable at room temperature.¹⁴ The size dependence of the spin splitting on both the energy and momentum also provides two controlling parameters for manipulating the spintronic devices. In addition to the large Rashba splitting, the Ag QWSs behave similarly to TI SSs in the energy region with a strong hybridization effect around the zone center (R1 state in the upper panel of Figure 2f), and provide better transport properties and much higher spin polarizations. The proposed NM/TI heterostructure would make real industrial applications more feasible than the TI itself.

CONCLUSIONS

In summary, we propose a new mechanism combining in-gap strong hybridization and spin-dependent scattering effects to manufacture the large Rashba-type splitting in NM QWSs. The calculated momentum separation of $\sim 0.18 \text{ \AA}^{-1}$ of the Ag QWS in the $\text{Ag/Bi}_2\text{Se}_3$ heterostructure is the largest one among all metal films based on non-metallic substrates. Our study has added metal QWSs to the family of materials that can produce large Rashba-type splittings. Furthermore, the induced spin polarization in the Ag QWS is nearly 100%, which is much higher than that in the TI SS itself. In addition to the large band splitting, high spin polarization and better transport properties, the NM QWS also avoids the difficulties of dealing with TI SSs or interfacial two-dimensional electron gases. We emphasize that the $\text{Ag/Bi}_2\text{Se}_3$ junction studied in this work is a model system for displaying the DSS-induced spin splitting in QWSs. We have performed similar calculations for $\text{Au/Bi}_2\text{Se}_3$ and $\text{Ag/Bi}_2\text{Te}_3$ and obtained similar results, demonstrating that various NM/TI heterostructures would be possible for fulfilling our proposed mechanism of high-efficiency spintronics. Recently, different types of NM/TI systems have been manufactured,^{57,58} and the first Datta-Das spin transistor has been realized.⁷ Our work thus invites experiments to realize our proposed mechanism.

ACKNOWLEDGEMENTS

This work was supported by the National Science Council, Academia Sinica and the National Tsing Hua University, Taiwan. We acknowledge Professors J Kwo, Tzay-Ming Hong, Chao-Cheng Kaun and Ching-Ray Chang for fruitful discussions. We also thank NCHC, CINC-NTU and NCTS, Taiwan, for technical supports.

- 1 Datta, S. & Das, B. Electronic analog of the electrooptic modulator. *Appl. Phys. Lett.* **56**, 665 (1990).
- 2 Žutić, I., Fabian, J. & Das Sarma, S. Spintronics: fundamentals and applications. *Rev. Mod. Phys.* **76**, 323–410 (2004).
- 3 Bychkov, Y. & Rashba, E. Properties of a 2d electron gas with lifted spectral degeneracy. *JETP Lett.* **39**, 78 (1984).
- 4 Nitta, J., Akazaki, T., Takayanagi, H. & Enoki, T. Gate control of spin-orbit interaction in an inverted $\text{In}_{0.53}\text{Ga}_{0.47}\text{As}/\text{In}_{0.52}\text{Al}_{0.48}\text{As}$ heterostructure. *Phys. Rev. Lett.* **78**, 1335–1338 (1997).
- 5 Murakami, S., Nagaosa, N. & Zhang, S.-C. Dissipationless quantum spin current at room temperature. *Science* **301**, 1348–1351 (2003).

- 6 Sinova, J., Culcer, D., Niu, Q., Sinitsyn, N. A., Jungwirth, T. & MacDonald, A. H. Universal intrinsic spin hall effect. *Phys. Rev. Lett.* **92**, 126603 (2004).
- 7 Chuang, P., Ho, S.-C., Smith, L., W., Sfigakis, F., Pepper, M., Chen, C.-H., Fan, J.-C., Griffiths, J. P., Farrer, I., Beere, H., E., Jones, G. A. C., Ritchie, D. A. & Chen, T.-M. All-electric all-semiconductor spin field-effect transistors. *Nat. Nano* **10**, 35–39 (2015).
- 8 Koo, H. C., Kwon, J. H., Eom, J., Chang, J., Han, S. H. & Johnson, M. Control of spin precession in a spin-injected field effect transistor. *Science* **325**, 1515–1518 (2009).
- 9 Wunderlich, J., Park, B.-G., Irvine, A. C., Zárbo, L. P., Rozkotová, E., Nemeč, P., Novák, V., Sinova, J. & Jungwirth, T. Spin hall effect transistor. *Science* **330**, 1801–1804 (2010).
- 10 LaShell, S., McDougall, B. A. & Jensen, E. Spin splitting of an Au(111) surface state band observed with angle resolved photoelectron spectroscopy. *Phys. Rev. Lett.* **77**, 3419–3422 (1996).
- 11 Koroteev, Y. u. M., Bihlmayer, G., Gayone, J. E., Chulkov, E. V., Blügel, S., Echenique, P. M. & Hofmann, P. h. Strong spin-orbit splitting on Bi surfaces. *Phys. Rev. Lett.* **93**, 046403 (2004).
- 12 Ast, C. R., Henk, J., Ernst, A., Moreschini, L., Falub, M. C., Pacilé, D., Bruno, P., Kern, K. & Grioni, M. Giant spin splitting through surface alloying. *Phys. Rev. Lett.* **98**, 186807 (2007).
- 13 Gierz, I., Suzuki, T., Frantzeskakis, E., Pons, S., Ostanin, S., Ernst, A., Henk, J., Grioni, M., Kern, K. & Ast, C. R. Silicon surface with giant spin splitting. *Phys. Rev. Lett.* **103**, 046803 (2009).
- 14 Yaji, K., Ohtsubo, Y., Hatta, S., Okuyama, H., Miyamoto, K., Okuda, T., Kimura, A., Namatame, H., Taniguchi, M. & Aruga, T. Large Rashba spin splitting of a metallic surface-state band on a semiconductor surface. *Nat. Commun.* **1**, 17 (2010).
- 15 Ishizaka, K., Bahramy, M. S., Murakawa, H., Sakano, M., Shimojima, T., Sonobe, T., Koizumi, K., Shin, S., Miyahara, H., Kimura, A., Miyamoto, K., Okuda, T., Namatame, H., Taniguchi, M., Arita, R., Nagaosa, N., Kobayashi, K., Murakami, Y., Kumai, R., Kaneko, Y., Onose, Y. & Tokura, Y. Giant Rashba-type spin splitting in bulk BiTeI. *Nat. Mater.* **10**, 521–526 (2011).
- 16 Eremeev, S. V., Nechaev, I. A., Koroteev, Y. M., Echenique, P. M. & Chulkov, E. V. Ideal two-dimensional electron systems with a giant Rashba-type spin splitting in real materials: surfaces of bismuth tellurohalides. *Phys. Rev. Lett.* **108**, 246802 (2012).
- 17 He, K., Hirahara, T., Okuda, T., Hasegawa, S., Kakizaki, A. & Matsuda, I. Spin polarization of quantum well states in Ag films induced by the Rashba effect at the surface. *Phys. Rev. Lett.* **101**, 107604 (2008).
- 18 Frantzeskakis, E., Pons, S., Mirhosseini, H., Henk, J., Ast, C. R. & Grioni, M. Tunable spin gaps in a quantum-confined geometry. *Phys. Rev. Lett.* **101**, 196805 (2008).
- 19 Bian, G., Zhang, L., Liu, Y., Miller, T. & Chiang, T.-C. Illuminating the surface spin texture of the giant-Rashba quantum-well system $\text{Bi}/\text{Ag}(111)$ by circularly polarized photoemission. *Phys. Rev. Lett.* **108**, 186403 (2012).
- 20 Dil, J. H., Meier, F., Lobo-Checa, J., Patthey, L., Bihlmayer, G. & Osterwalder, J. Rashba-type spin-orbit splitting of quantum well states in ultrathin Pb films. *Phys. Rev. Lett.* **101**, 266802 (2008).
- 21 Slomski, B., Landolt, G., Bihlmayer, G., Osterwalder, J. & Dil, J. H. Tuning of the Rashba effect in Pb quantum wellstates via a variable scattering barrier. *Sci. Rep.* **3**, 1963 (2013).
- 22 Mathias, S., Ruffing, A., Deicke, F., Wiesenmayer, M., Sakar, I., Bihlmayer, G., Chulkov, E. V., Koroteev, Y. u. M., Echenique, P. M., Bauer, M. & Aeschlimann, M. Quantum-well-induced giant spin-orbit splitting. *Phys. Rev. Lett.* **104**, 066802 (2010).
- 23 Lüth, H. *Interfaces and Thin Films* 6th edn Springer: Berlin, Heidelberg, (2015).
- 24 Kane, C. L. & Mele, E. J. Z2 topological order and the quantum spin Hall effect. *Phys. Rev. Lett.* **95**, 146802 (2005).
- 25 Fu, L., Kane, C. L. & Mele, E. J. Topological insulators in three dimensions. *Phys. Rev. Lett.* **98**, 106803 (2007).
- 26 Bernevig, B. A., Hughes, T. L. & Zhang, S.-C. Quantum spin hall effect and topological phase transition in HgTe quantumwells. *Science* **314**, 1757–1761 (2006).
- 27 König, M., Wiedmann, S., Brüne, C., Roth, A., Buhmann, H., Molenkamp, L. W., Qi, X.-L. & Zhang, S.-C. Quantum spin hall insulator state in HgTe quantum wells. *Science* **318**, 766–770 (2007).
- 28 Hsieh, D., Qian, D., Wray, L., Xia, Y., Hor, Y. S., Cava, R. J. & Hasan, M. Z. A topological Dirac insulator in a quantum spin hall phase. *Nature* **452**, 970–974 (2008).
- 29 Xia, Y., Qian, D., Hsieh, D., Wray, L., Pal, A., Lin, H., Bansil, A., Grauer, D., Hor, Y. S., Cava, R. J. & Hasan, M. Z. Observation of a large-gap topological-insulator class with a single Dirac cone on the surface. *Nat. Phys.* **5**, 398–402 (2009).
- 30 Zhang, T., Cheng, P., Chen, X., Jia, J.-F., Ma, X., He, K., Wang, L., Zhang, H., Dai, X., Fang, Z., Xie, X. & Xue, Q.-K. Experimental demonstration of topological surface states protected by time-reversal symmetry. *Phys. Rev. Lett.* **103**, 266803 (2009).
- 31 Zhang, H., Liu, C.-X., Qi, X.-L., Dai, X., Fang, Z. & Zhang, S.-C. Topological insulators in Bi_2Se_3 , Bi_2Te_3 and Sb_2Te_3 with a single Dirac cone on the surface. *Nat. Phys.* **5**, 438–442 (2009).
- 32 Kato, Y. K., Myers, R. C., Gossard, A. C. & Awschalom, D. D. Observation of the spin hall effect in semiconductors. *Science* **306**, 1910–1913 (2004).
- 33 Moore, J. E. The birth of topological insulators. *Nature* **464**, 194–198 (2010).
- 34 Hasan, M. Z. & Kane, C. L. Colloquium: topological insulators. *Rev. Mod. Phys.* **82**, 3045–3067 (2010).
- 35 Qi, X.-L. & Zhang, S.-C. Topological insulators and superconductors. *Rev. Mod. Phys.* **83**, 1057–1110 (2011).
- 36 Varykhalov, A., Sánchez-Barriga, J., Shikin, A. M., Gudat, W., Eberhardt, W. & Rader, O. Quantum cavity for spin due to spin-orbit interaction at a metal boundary. *Phys. Rev. Lett.* **101**, 256601 (2008).

- 37 Yokoyama, T., Tanaka, Y. & Nagaosa, N. Giant spin rotation in the junction between a normal metal and a quantum spin Hall system. *Phys. Rev. Lett.* **102**, 166801 (2009).
- 38 Neupane, M., Richardella, A., Sánchez-Barriga, J., Xu, S. Y., Alidoust, N., Belopolski, I., Liu, C., Bian, G., Zhang, D., Marchenko, D., Varykhalov, A., Rader, O., Leandersson, M., Balasubramanian, T., Chang, T.-R., Jeng, H.-T., Basak, S., Lin, H., Bansil, A., Samarth, N. & Hasan, M. Z. Observation of quantum-tunnelling-modulated spin texture in ultrathin topological insulator Bi_2Se_3 films. *Nat. Commun.* **5**, 3841 (2014).
- 39 Yazev, O. V., Moore, J. E. & Louie, S. G. Spin polarization and transport of surface states in the topological insulators Bi_2Se_3 and Bi_2Te_3 from first principles. *Phys. Rev. Lett.* **105**, 266806 (2010).
- 40 Zhu, Z.-H., Veenstra, C. N., Levy, G., Ubaldini, A., Syers, P., Butch, N. P., Paglione, J., Haverkort, M. W., Elfimov, I. S. & Damascelli, A. Layer-by-layer entangled spin-orbital texture of the topological surface state in Bi_2Se_3 . *Phys. Rev. Lett.* **110**, 216401 (2013).
- 41 Blöchl, P. E. Projector augmented-wave method. *Phys. Rev. B* **50**, 17953–17979 (1994).
- 42 Kresse, G. & Joubert, D. From ultrasoft pseudopotentials to the projector augmented-wave method. *Phys. Rev. B* **59**, 1758–1775 (1999).
- 43 Kresse, G. & Hafner, J. *Ab initio* molecular dynamics for open-shell transition metals. *Phys. Rev. B* **48**, 13115–13118 (1993).
- 44 Kresse, G. & Furthmüller, J. Efficient iterative schemes for *ab initio* total-energy calculations using a plane-wave basis set. *Phys. Rev. B* **54**, 11169–11186 (1996).
- 45 Perdew, J. P., Burke, K. & Ernzerhof, M. Generalized gradient approximation made simple. *Phys. Rev. Lett.* **77**, 3865–3868 (1996).
- 46 Popović, D., Reinert, F., Hufner, S., Grigoryan, V. G., Springborg, M., Cercellier, H., Fagot-Revurat, Y., Kierren, B. & Malterre, D. High-resolution photoemission on Ag/Au (111): spin-orbit splitting and electronic localization of the surface state. *Phys. Rev. B* **72**, 045419 (2005).
- 47 Cercellier, H., Didiot, C., Fagot-Revurat, Y., Kierren, B., Moreau, L., Malterre, D. & Reinert, F. Interplay between structural, chemical, and spectroscopic properties of Ag/Au(111) epitaxial ultrathin films: a way to tune the Rashba coupling. *Phys. Rev. B* **73**, 195413 (2006).
- 48 Ma, Y., Dai, Y., Wei, W., Li, X. & Huang, B. Emergence of electric polarity in BiTeX (X = Br and I) monolayers and the giant Rashba spin splitting. *Phys. Chem. Chem. Phys.* **16**, 17603 (2014).
- 49 Li, X., Dai, Y., Ma, Y., Wei, W., Yu, L. & Huang, B. Prediction of large-gap quantum spin hall insulator and Rashba-Dresselhaus effect in two-dimensional g-TIA (A = N, P, As, and Sb) monolayer films. *Nano Res.* **8**, 2954 (2015).
- 50 Bahramy, M. S., Yang, B. J., Arita, R. & Nagaosa, N. Emergence of non-centrosymmetric topological insulating phase in BiTeI under pressure. *Nat. Commun.* **3**, 679 (2012).
- 51 Ojeda-Aristizabal, C., Fuhrer, M. S., Butch, N. P., Paglione, J. & Appelbaum, I. Towards spin injection from silicon into topological insulators: Schottky barrier between Si and Bi_2Se_3 . *Appl. Phys. Lett.* **101**, 023102 (2012).
- 52 Wei, C. M. & Chou, M. Y. Effects of the substrate on quantum well states: a first-principles study for Ag/Fe(100). *Phys. Rev. B* **68**, 125406 (2003).
- 53 Menschikova, T. V., Otrokov, M. M., Tsirkin, S. S., Samorokov, D. A., Bebeva, V. V., Ernst, A., Kuznetsov, V. M. & Chulkov, E. V. Band structure engineering in topological insulator based heterostructures. *Nano Lett.* **13**, 6064–6069 (2013).
- 54 King, P. D. C., Hatch, R. C., Bianchi, M., Ovsyannikov, R., Lupulescu, C., Landolt, G., Slomski, B., Dil, J. H., Guan, D., Mi, J. L., Rienks, E. D. L., Fink, J., Lindblad, A., Svensson, S., Bao, S., Balakrishnan, G., Iversen, B. B., Osterwalder, J., Eberhardt, W., Baumberger, F. & Hofmann, P. h. Large tunable Rashba spin splitting of a two-dimensional electron gas in Bi_2Se_3 . *Phys. Rev. Lett.* **107**, 096802 (2011).
- 55 Zhu, Z.-H., Levy, G., Ludbrook, B., Veenstra, C. N., Rosen, J. A., Comin, R., Wong, D., Dosanjh, P., Ubaldini, A., Syers, P., Butch, N. P., Paglione, J., Elfimov, I. S. & Damascelli, A. Rashba spin-splitting control at the surface of the topological insulator Bi_2Se_3 . *Phys. Rev. Lett.* **107**, 186405 (2011).
- 56 Bahramy, M. S., King, P. D. C., de la Torre, A., Chang, J., Shi, M., Patthey, L., Balakrishnan, G., Hofmann, P. h., Arita, R., Nagaosa, N. & Baumberger, F. Emergent quantum confinement at topological insulator surfaces. *Nat. Commun.* **3**, 1159 (2012).
- 57 He, Q. L., Lai, Y. H., Lu, Y., Law, K. T. & Sou, I. K. Surface reactivity enhancement on a Pd/ Bi_2Te_3 heterostructure through robust topological surface states. *Sci. Rep.* **3**, 2497 (2013).
- 58 Mellnik, A. R., Lee, J. S., Richardella, A., Grab, J. L., Mintun, P. J., Fischer, M. H., Vaezi, A., Manchon, A., Kim, E.-A., Samarth, N. & Ralph, D. C. Spin-transfer torque generated by a topological insulator. *Nature* **511**, 449–451 (2014).



This work is licensed under a Creative Commons Attribution 4.0 International License. The images or other third party material in this article are included in the article's Creative Commons license, unless indicated otherwise in the credit line; if the material is not included under the Creative Commons license, users will need to obtain permission from the license holder to reproduce the material. To view a copy of this license, visit <http://creativecommons.org/licenses/by/4.0/>

© The Author(s) 2016

Supplementary Information accompanies the paper on the NPG Asia Materials website (<http://www.nature.com/am>)